

Theoretical Investigations on Adsorption of NO on Copper Exchanged Zeolites (Cu-ZSM-5)

BY GEORGE SCHOENDORFF

Abstract

Adsorption of NO on copper exchanged ZSM-5 is investigated using *ab initio* methods. Cluster models, ranging from 1T to 5T (T is silicon or aluminum), are used to represent the structure of zeolites. Equilibrium structures are calculated at the HF and DFT theory levels. Relative energies among different adsorption complexes are calculated.

Introduction

“Acid rain” (or so-called acid deposition) is a broad term used to describe both wet and dry ways that acid falls out of the atmosphere. Acid rain has received worldwide attention during the past thirty years since

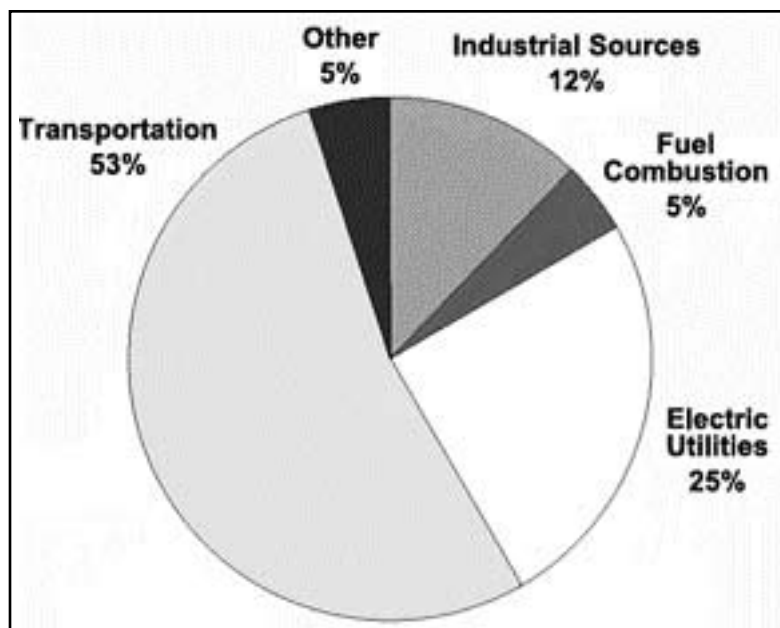


Figure 1: NO_x emissions from the United States in 1998.¹

it deteriorates our vulnerable environment and leads to serious health problems.¹⁻⁴ Wet deposition refers to acidic rain, fog, and snow. Dry deposition refers to acidic gases absorbing on surfaces and particles settling out. The direct effect of acid deposition is to harm the natural environment, including plants, aquifers, and aquatic organisms. Another important effect, but frequently ignored by many people, results from chemical reactions with existing minerals in the soil to generate soluble toxic metal ions, which eventually enter our bodies *via* foods and/or drinking water. Accumulation of such toxic metals can lead to serious health problems.¹⁻³

Tremendous efforts, including labor and money, have been spent in controlling acid rain. However, it is neither an easy task nor a short-term fight. NO_x, a mixture of NO and NO₂, is one major contributor to acid rain¹⁻⁴ and is emitted primarily in exhaust fumes from millions of automobiles.² In 1998, this accounted for 53% of NO_x emissions in the United States (Figure 1). In 2000, the total emissions of NO_x in the United States was 5.11 million tons.¹ It is of interest and importance, therefore, to develop a powerful catalyst to selectively reduce NO_x and eventually to reduce the damage caused to humans and environments.⁵⁻⁸

pore ZSM-5 zeolite has attracted a lot of attention. Because of small pore size and its uniform distribution, the internal surface developed by the porous channels is much larger than the external surface. The higher ratio of internal to external surface area (about 4:1) leads to its higher activity and selectivity.^{12,13}

Due to the existence of the aluminum in the TO_4 unit, oxygen atoms adjacent to the aluminum show the partial negative charges, which can be balanced by external cations. Copper exchanged ZSM-5 (Cu-ZSM-5), a new derivative of ZSM-5, is the most active catalyst for the direct decomposition of NO_x to date.^{14,15} Cu-ZSM-5 has adsorption properties similar to ZSM-5.¹² The ratio of internal surface area to external surface area is even larger than that of ZSM-5. The study of pore size distribution demonstrates that Cu-ZSM-5 represents a well-defined distribution with main micropore size at 0.7 nm with a limit of 2 nm. Experimental studies have shown that

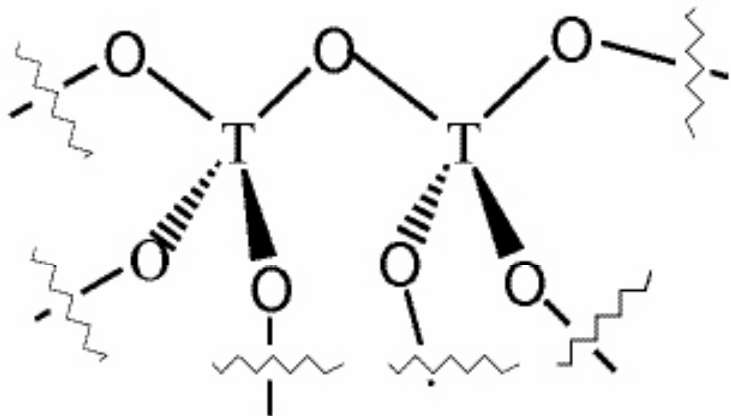


Figure 2: The tetrahedral TO_4 unit in zeolites.

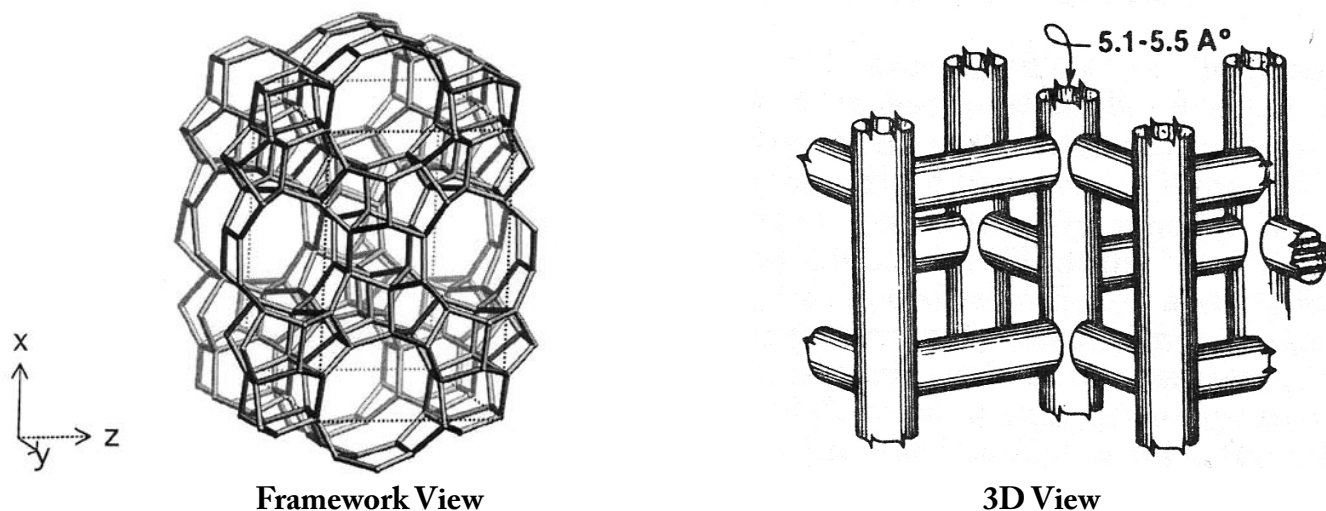


Figure 3: The structure of zeolite (MFI type).^{12,13}

Cu-ZSM-5, rather than ZSM-5 or naked copper cation, exhibits high activity in decomposing NO_x into N_2 and O_2 , major components of the air.^{16,17} However, the detailed adsorption-decomposition reaction mechanisms remain unknown from the experimental investigations.

The computational tool is an alternative and/or support to the experimental research, but theoretical studies (*ab initio* calculations) of bulky zeolites are limited by computer resources. With the recent development in theoretical methods, two affordable approximations, the cluster model and the embedded cluster model, can be used to represent the interaction between adsorbed molecules (adsorbate) and zeolite fragments, as well as between zeolite fragments and the whole framework.¹⁸⁻²³

The mechanism of adsorption-decomposition of NO on Cu-ZSM-5 is complicated and involves many steps.²⁴ This study focused only on the adsorption of NO on Cu-ZSM-5, the first step in the adsorption-decomposition process. Only chemically bonded adsorption complexes may be stable enough to allow subsequent decomposition reactions. There are three possible structures of the NO-Cu-ZSM-5 adsorption complex. *Ab initio* calculations of the structure of these complexes were performed to determine possible adsorption complexes and energy barriers.

Approaches

Cluster model was used in this project to simulate the zeolite structures. Zeolite is treated as a very small neutral cluster cut out of the bulky crystal structure. Hydrogen atoms terminate the resulting dangling bonds at the boundary.²⁰ Since the cluster model takes only a very small part of the zeolite structure, two important deficiencies of cluster models exist.²⁹ First, the cluster model is different from the zeolite structure because atoms near the cluster boundary, arbitrarily terminated by H, are in different electronic environments. The second is potential deficiency. A potential is generated from the long-range electrostatic forces between the cluster model and the zeolite framework, which is missing in cluster calculations.

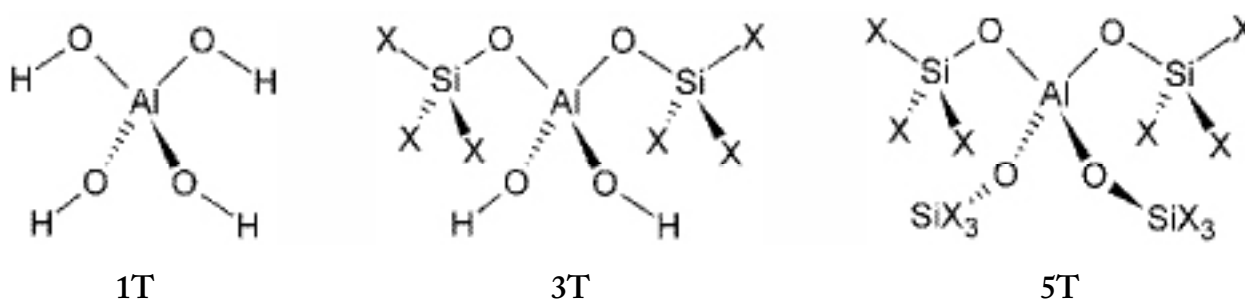


Figure 4: The cluster models (X = H or OH).

Results obtained from cluster model investigation may give us a chance to examine the usage of embedded cluster model. A recently developed embedded cluster model method can be used to avoid/alleviate aforementioned problems without significantly increasing the computational costs.³⁰⁻³²

Computational Details

Full optimizations of cluster models, from 1T to 5T models (Figure 4), were performed at the Hartree Fock (HF)25 and then the Density Functional Theory (DFT)27 levels with the 6-31G(d) basis set using the *ab initio* suite of GAMESS package.²⁸ Additionally, MacMolPlt, a 3D visualization package, was used to view the optimized geometries.³³ All calculations were performed on a Mac Power G5 cluster.

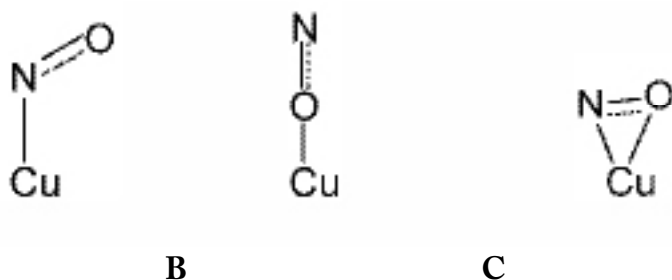


Figure 5: Three possible NO-Cu adsorption complexes.

Results

There are three possible ways for NO to adsorb on Cu-ZSM-5 (Figure 5). The first possibility is the formation of a bond between Cu and N to give the Cu-N-O adsorption complex (A). Alternatively, a bond between Cu and O could form, yielding the Cu-O-N adsorption complex (B). The remaining possibility is for Cu to bond to both N and O to make a Cu-N-O ring structure (C). Geometries optimized at the HF level and at the DFT

level are listed in Table 1 and 2, respectively. Due to the substitution of Si by Al in the zeolite framework, oxygen

atoms next to Al are partially negatively charged. As a result, Cu cations are bound to balance this negative charge. Since NO is a polar molecule and the dipole moment points to N from O, different binding type should affect bonding in NO, even the relative stabilities of different adsorption complexes.

Complex A must have a shorter Cu-O bond length than B because the partially negative charges on O in B are shared between Cu and N. As a result, the N-O bond strength is decreased. Complex C will show the longest N-O distance because Cu forms bonds to both N and O. Because both N and O share Cu, it is expected that Cu-N bond is weaker than that in complex A but Cu-O bond is stronger than that in complex B. Both HF and DFT results show the same tendency. At the DFT level, molecular NO was calculated to have a bond length of 1.1589 Å. DFT results in Table 2 show that N-O length in structure A is the closest to that of molecular NO while that in structure C is about 0.08 – 0.09 Å longer.

From Table 1 and 2, it is also found that, with the increase in cluster size, geometrical parameters of cluster framework (e.g. Cu-Al distance) may change drastically. A similar observation is found when a different terminal group is used. Compared with the change inside of the zeolite framework, changes in bonding between zeolite and adsorbate are smaller (usually less than 0.02 Å) but not neglected.

HF shows that the optimized geometries have C_{2v} or C_s symmetry since the dihedral angle OCuNO is always zero. Compared with DFT results, HF can predict the conformations of B and C qualitatively correct, though HF always overestimates the bond lengths. However, the A complex displays a quite different dihedral angle near 90° in HF and DFT studies: in small clusters, DFT results support an out-of-plane structure with the C₁ symmetry. With the increasing size of the cluster model, such stable structures vanish. It may suggest that in this study both the cluster size and electron correlation could be important factors. The CuNO angle in the A complex also varies between the HF and DFT geometries.

The HF geometries always predict a 180° bond angle. Once again, this is due to the symmetry of the optimized HF geometries. The CuNO bond angle in the DFT structures is near 150°. This 150° bond angle occurs with the

	1T			3T-H			3T-OH			5T-H		
Adsorption type	A	B	C	A	B	C	A	B	C	A	B	C
Distance (Å)												
Al-Cu	2.8477	2.8289	2.8443	2.7950	2.7836	2.7832	2.8441	2.8393	2.8282	2.7851	2.7702	2.7755
Cu-N	1.8957		1.9299	1.9272		1.9972	1.9444		2.0660	1.9387		2.0237
Cu-O		2.0886	1.9337		2.1009	1.9800		2.0978	2.0197		2.1052	1.9978
N-O	1.1205	1.1287	1.1651	1.1188	1.1293	1.1548	1.1180	1.1288	1.1480	1.1184	1.1294	1.1516
Bond angle (degrees)												
Cu-N-O	180.0		72.6	180.0		72.4	180.0		71.5	180.0		72.1
Cu-O-N		180.0	72.3		180.0	73.9		180.0	75.9		180.0	74.6
O-Cu-N	141.0		118.9	139.7		119.1	140.7		120.6	139.7		119.5
O-Cu-O		140.7	127.7		139.6	125.9		140.6	127.2		139.4	126.0
Dihedral angle (degrees)												
O-Cu-N-O	0.0	0.0	0.0	0.0	0.0	0.0	0.0	0.0	0.0	0.0	0.0	0.0

Table 1: Distances and bond angles calculated at the HF level with the 6-31G(d) basis set.

90° dihedral angle in these structures. However, this bond angle becomes 180° when the dihedral angle is 0.0° in the larger clusters. The variations of the CuNO angle and the dihedral angle in the DFT structures always occur together. Therefore, when C_{2v} or C_s is broken in the small DFT clusters, it is because O from NO lies roughly 30° outside the C_s plane.

The relative energies of the adsorption complexes at the HF level show little variation among the 1T and 3T clusters (Table 3). The calculated energies at the HF level indicate that adsorption type A is the most stable and, therefore

Adsorption type	1T			3T-H			3T-OH			5T-H		
	A	B	C	A	B	C	A	B	C	A	B	C
Distance (Å)												
Al-Cu	2.7793	2.8323	2.7706	2.7898	2.7763	2.7706	2.8186	2.8082	2.8010	2.8011	2.7571	2.7585
Cu-N	1.7191		1.8351	1.7241		1.8351	1.7095		1.8395	1.7237		1.8364
Cu-O		1.7589	1.8625		1.7667	1.8625		1.7683	1.8629		1.7694	1.8648
N-O	1.1777	1.1880	1.2421	1.1759	1.1862	1.2421	1.1723	1.1839	1.2397	1.1707	1.1854	1.2410
Bond angle (degrees)												
Cu-N-O	149.8		71.9	149.2		71.6	180.0		71.5	180.0		71.7
Cu-O-N		180.0	68.6		180.0	69.2		180.0	69.4		180.0	69.2
O-Cu-N	123.5		114.9	139.0		115.5	139.6		116.0	139.5		114.5
O-Cu-O		140.3	126.2		138.8	122.3		139.4	123.0		138.6	123.2
Dihedral angle (degrees)												
O-Cu-N-O	88.5	0.0	0.0	93.8	0.0	0.0	0.0	0.0	0.0	0.0	0.0	0.0

Table 2: Distances and bond angles calculated at the DFT level with the 6-31G(d) basis set.

Adsorption Type	1T	3T-H	3T-OH	5T-H
HF//HF				
A	0.0	0.0	0.0	0.0
B	5.52	4.27	3.94	3.86
C	4.56	6.34	7.99	6.77
DFT//DFT				
A	0.0	0.0	0.0	4.45
B	28.49	24.89	25.06	19.46
C	6.55	4.89	4.96	0.0

Table 3: Relative energies (kcal/mol) calculated using 6-31G(d) basis set.

the most likely adsorption type. The B and C types are relatively closer in energy. DFT energies, however, differ significantly from the HF energies. The 1T and 3T clusters still indicated type A as the most stable complex and B is significantly higher in energy than C. The substantial differences in energies at the DFT level demonstrate the importance of electron correlation in these calculations. Given the DFT energies, type B is clearly the least stable of the adsorption complexes. The cluster size also contributes to the difference in the DFT calculations. 1T and 3T cluster models indicate that the A type is the most stable, followed by the B type. When the cluster is enlarged to 5T, though, the C type is the most stable followed by the A type.

Discussion

The most obvious conclusion from this data is that the cluster size has a significant impact on the energies of the complexes as well as on the geometries. If only small clusters are used, then the A type adsorption complex would appear to be the most stable. However, framework effects from the larger 5T zeolite cluster seem to increase the stability of the C type adsorption complex. DFT data from the 5T (-H terminated) cluster model indicate that type C is in fact the favored adsorption mechanism, contrary to the established trend from smaller clusters. Type C, with its longer N-O bond length, would be better able to dissociate NO into N and O ions or radicals.

In addition to the effects of the cluster size, the level of theory (DFT vs. HF) also impacts the results. Electron correlation from the DFT calculations contributes to a large increase in the relative energy of the B complex. From HF energies alone, it is not clear whether type B or type C is the most stable. DFT results, however, show a clear difference in energy between these two adsorption complexes. Type B, then, is clearly the least stable complex. Type C, on the other hand, appears to be the most stable given a large cluster size.

The results in Table 3 also indicate a difference between –H termination and –OH termination. Though two clusters may have the same number of tetrahedral units, the type of termination used still impacts the results. Changing the cluster from –H terminated to –OH terminated can greatly change the electron distribution in the zeolite framework and, further, change the binding of the adsorbate.

With only one type of cluster contradicting the stability of the A type mechanism, it is unclear whether this result is an anomaly. Therefore, it is necessary to obtain DFT results for other large clusters – namely the 5T –OH terminated and 10T clusters. If type C is the most stable complex in these larger clusters, then it will be clear that small clusters give qualitatively incorrect results.

Acid rain is a serious problem that affects everyone. It can cause aesthetic damage to paints and other coatings. More importantly, it affects the environment by acidifying soils and aquifers. Changes in pH are harmful to aquatic animals by interfering with biological processes and reducing the amount of available calcium carbonate for shells. In addition, acid in the soil can react with metals bound up in minerals and cause them to be released into drinking water. Many of these metals are toxic to humans and other animals. Additionally, many acidic gases -- in particular nitrogen oxides -- are greenhouse gases. Although the amount of these emissions is small compared to the production of CO₂, they still contribute to climate change. Acidic gases are produced through both natural means such as volcanism as well as through the burning of fossil fuels.

Any technology that reduces the production of acidic gases will greatly benefit people and the environment. This includes alternative energy sources such as solar or wind power, alternative fuels such as hydrogen or biofuels, or catalysts that reduce acidic gases to harmless molecules. So far, copper exchanged zeolite is one of the most promising catalysts that shows stronger catalytic capability over NO from small-scale experimental studies. However, before it is used on a large scale, it is necessary to understand how and why it works and whether it can be improved. If the reaction mechanism for the reduction of NO on zeolite is understood, it may be possible to design better catalysts that work in a wider range of circumstances.

References

1. <http://www.epa.gov/acidrain>
2. <http://www.ec.gc.ca/acidrain/acidfact.html>
3. <http://www.policyalmanac.org/>
4. Friedman, S. M. and Friedman, K. A. "Reporting on the Environment: A Handbook for Journalists," the Asian Forum of Environmental Journalists in cooperation with The United Nations Economic and Social Commission for Asia and the Pacific. Bangkok, Thailand. **1988**.
5. Shelef, M. *Chem. Rev.* **1995**, 95, 209.
6. Henao, J. D.; Cordoba, L. F.; de Correa, C. M. *J. Mol. Catal. A.* **2004**, 207, 195.
7. Myers, A. L. *Langmuir.* **2002**, 18, 10261.
8. Magnacca, G.; Morterra, C. *Phys. Chem. Chem. Phys.* **2000**, 2, 3903.
9. Arbuznikov, A.; Vasilyev, V.; Goursot, A. *Surface Science.* **1998**, 397, 395.
10. Bonneviot, L.; Kaliaguine, S. "Zeolites: A Refined Tool for Designing Catalytic Sites," *Elsevier*. Amsterdam, Holland. **1995**.
11. Chen, N. W.; Garwood, W. E.; Dwyer, F. G. "Shape Selective Catalysis in Industrial Applications," 2nd Revised and Expanded Edition. Marcel Dekker, New York. **1996**.

12. Gervasini, A. *J. Appl. Catal. A*. **1999**, *180*, 71.
13. <http://www.iza-structure.org/databases/>
14. Li, Y.; Hall, W. K. *J. Catal.* **1991**, *129*, 202.
15. Iwamoto, M.; Yahiro, H.; Tanda, K.; Mizuno, N.; Mine, Y.; Kagawa, S. *J. Phys. Chem.* **1991**, *95*, 3727.
16. Trout, B. L.; Chakraborty, A. K.; Bell, A. T. *J. Phys. Chem.* **1996**, *100*, 17582.
17. Kuroda, Y.; Yoshikawa, Y.; Kumashiro, R.; Nagao, M. *J. Phys. Chem. B*. **1997**, *101*, 6497.
18. Brand, V. H.; Redondo, A.; Hay, P. J. *J. Mol. Catal. A*. **1997**, *121*, 45.
19. Vollmer, J.; Stefanovich, E. V.; Truong, T. N. *J. Phys. Chem. B*. **1999**, *103*, 9415.
20. Brandle, M.; Sauer, J. *J. Mol. Catal. A*. **1997**, *119*, 19.
21. Ketrat, S.; Limtrakul, J. *Int. J. Quantum Chem.* **2003**, *94*, 333.
22. Arstad, B.; Kolboe, S.; Swang, O. *J. Phys. Chem. B*. **2004**, *108*, 2300.
23. Soscum, H.; Castellano, O.; Hernandez, J. *J. Phys. Chem. B*. **2004**, *108*, 5620.
24. Schneider, W. F.; Hass, K. C.; Ramprasad, R.; Adams, J. B. *J. Phys. Chem.* **1997**, *101*, 4353.
25. Roothan, C. C. *J. Rev. Mod. Phys.*, 1951, *23*, 69; Pople J. A.; Nesbet, R. K. *J. Chem. Phys.* **1954**, *22*, 571; R. McWeeny R.; Dierksen, G. *J. Chem. Phys.* **1968**, *49*, 4852.
26. Head-Gordon, M.; Pople, J. A.; Frisch, M. *J. Chem. Phys. Lett.* **1988**, *153*, 503; Frisch, M. J.; Head-Gordon, M.; Pople, J. A. *Chem. Phys. Lett.* **1990**, *166*, 275; Frisch, M. J.; Head-Gordon, M.; Pople, J. A. *Chem. Phys. Lett.* **1990**, *166*, 281; Head-Gordon, M.; Head-Gordon, T. *Chem. Phys. Lett.* **1994**, *220*, 122; Moller, C.; Plesset, M. S. *Phys. Rev.* **1934**, *46*, 618; Saebo S.; Almlof, J. *Chem. Phys. Lett.* **1989**, *154*, 83.
27. Dunlap, B. I. *J. Chem. Phys.* **1983**, *78*, 3140; Dunlap, B. I. *J. Mol. Struct. (Theochem)*. **2000**, *529*, 37.
28. Schmidt, M. W.; Baldrige, K. K.; Boatz, J. A.; Elbert, S. T.; Gordon, M. S.; Jensen, J. H.; Koseki, S.; Matsunaga, N.; Nguyen, K. A.; Su, S.; Windus, T. L.; Dupuis, M.; Montgomery, J. A. *J. Comput. Chem.* **1993**, *14*, 1347.
29. Nichlas, J. B.; Hess, A. C. *J. Am. Chem. Soc.* **1994**, *116*, 5428-5436.
30. Shoemaker, J. R.; Burggral, L. W.; Gordon, M. S. *J. Phys. Chem. A*. **1999**, *103*, 3245.
31. Carmer, C. S.; Weiner, B.; Frenklench, M. *J. Chem. Phys.* **1993**, *99*, 1356.
32. Maseras, F.; Morokuma, K. *J. Comput. Chem.* **1995**, *16*, 1170.
33. Bode, B. M.; Gordon, M. S. *J. Mol. Graphics Mod.* **1998**, *16*, 133.
34. Hayes, N. W.; Joyner, R. W.; Shapiro, E. S. *App. Cat. B*. **1996**, *8*, 343.